Magnetoelectric coupling dependent on ferroelectric switching paths in two-dimensional perovskite multiferroics

Xiaofan Shen,[1] Qunyong Luo,[1] Zongshuo Wu [ORCID],[1] Ying Zhou,[1] Jianli Wang,[1] Junting Zhang [ORCID],[1,*]
Jie Su,[2,†] and Xiaomei Lu [ORCID][3]

[1]*School of Materials Science and Physics, China University of Mining and Technology, Xuzhou 221116, China*
[2]*School of Electronic and Information Engineering, Qingdao University, Qingdao 266071, China*
[3]*National Laboratory of Solid State Microstructures and Physics School, Nanjing University, Nanjing 210093, China*

Two-dimensional (2D) multiferroics have attracted considerable interest since the recent discovery of 2D ferroelectricity and ferromagnetism in van der Waals materials. Here we show the universality of 2D multiferroics in the Ca-based double-perovskite bilayer system and the transition of magnetization that is dependent on the ferroelectric switching paths by combining symmetry analysis and first-principles calculation. We demonstrate that although both the switching of rotation and tilt distortion can lead to polarization reversal, only the latter can cause a change in the direction of magnetization. The breaking of the inversion symmetry correlation between the initial and final polarization states is the key to achieve the transition of magnetization caused by polarization reversal. The ferroelectric switching that reverses tilt distortion via multistep switching generally has the lowest energy barrier, providing the feasibility of controlling magnetization by an electric field.

DOI: 10.1103/PhysRevB.103.L220406

When a bulk crystal is reduced to two dimensions (2D), exotic electronic phases tend to emerge, resulting in unique physical properties that differ from its bulk [1–3]. Symmetry breaking caused by dimensionality reduction may play a key role in the emergence of new functions of 2D materials [2,4]. For example, spatial inversion symmetry breaking in 2D transition-metal dichalcogenides provides a basis for exploring their applications in piezoelectricity and valleytronics [5,6]. At present, 2D materials are mostly found in van der Waals materials, whose 2D building blocks retain their structural and chemical bond characteristics [7]. Recently, the successful growth of the freestanding perovskite oxides down to the monolayer limit provides a great opportunity to explore new functions of 2D materials beyond van der Waals materials [8,9]. Importantly, the coupling between lattice, charge, orbital, and spin degrees of freedom may induce exotic correlated electronic phases in 2D perovskite oxides [9,10].

Octahedral rotation distortion is very common in perovskite bulks but without breaking the spatial inversion symmetry [11]. However, recent studies have shown that when the perovskite bulk is reduced to 2D, a special type of octahedral rotation can break the spatial inversion symmetry [12,13], similar to the layered perovskite oxides [14–16]. This is promising to motivate research on the functional properties of 2D perovskites based on inversion symmetry breaking, such as ferroelectricity, piezoelectricity, chirality, valleytronics, and multiferroics [17–20]. Recently, we demonstrated that the 2D perovskite multiferroics can be achieved by extending to a magnetic double-perovskite (DP) bilayer, in which

the switchable polarization is coupled with magnetization via octahedral rotation [13]. However, several key issues remain to be addressed: (1) What are the universal results of this 2D system? (2) Are other low-energy ferroelectric switching paths possible? (3) What is the transition of magnetization along different switching paths?

In this Letter we choose a variety of $3d$-$4d$ and $3d$-$5d$ combinations of transition-metal ions for the designed 2D system with the formula $A_3BB'O_7$ (A=Ca, Sr), which contains the bilayers of 91 existing DP materials. We systematically investigate their structural, electronic, ferroelectric, and magnetic properties by using symmetry analysis and first-principles calculation (more details are given in the Supplemental Material [21]). The influence of Hubbard parameter U is discussed, and then some universal results are summarized. The symmetry correlation between the initial and final polarization states is analyzed to explain the transition of the magnetization direction along different ferroelectric switching paths. We demonstrate that although both the switching of rotation and tilt distortion can lead to polarization reversal, only the latter can break the inversion symmetry correlation, resulting in the reversal of the in-plane magnetization.

Considering the possible structural reconstruction caused by dimensionality reduction, we first examined the ground-state phases of all bilayers by using the structure search method. Starting from the prototype phase of the bilayers, it forms a $\sqrt{2} \times \sqrt{2} \times 2$ perovskite supercell due to the most common rock-salt-type arrangement of magnetic ions [22]. Previous study has shown that its three modes of octahedral rotation—in-phase rotation (IR), out-of-phase rotation (OR), and tilt—are all dynamically unstable [13]. Our tests show that only the freezing of these octahedral rotation modes can reduce the energy of the system (see Fig. S1 [21]). In
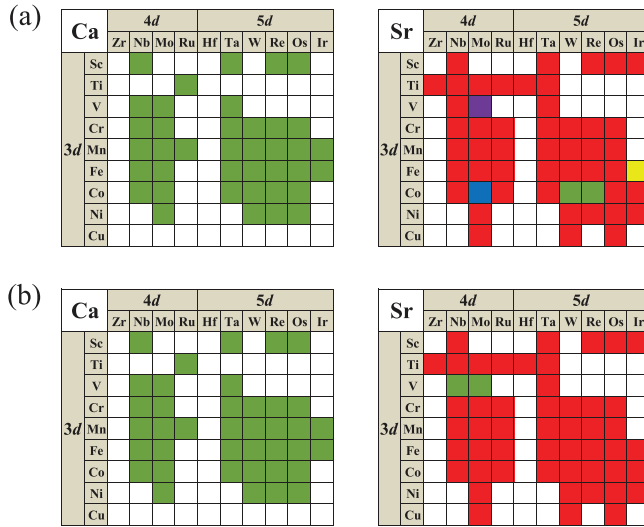
FIG. 1. Octahedral rotation types of the Ca-based and Sr-based bilayers with effective U values of (a) $U_{3d} = 4$ eV, $U_{4d/5d} = 1$ eV, and (b) $U_{3d} = 2$ eV, $U_{4d/5d} = 0$ eV. Color-filled squares represent the corresponding octahedral rotation types: $a^-a^-c^+$ (green), $a^-a^-c^-$ (red), $a^-b^0c^0$ (purple), $a^-b^0c^+$ (blue), and $a^0a^0c^-$ (yellow).

order to determine the ground-state structure, we analyzed the structural symmetry caused by various types of octahedral rotation and then calculated the energy of each structural phase.

For all the Ca-based bilayers, the ground-state structures have the $a^-a^-c^+$ type octahedral rotation (in the Glazer notation), independent of the U values used [see Figs. 1(a) and 1(b)]. Phonon dispersion and *ab initio* molecular dynamics simulation confirm the dynamic and thermal stability of this ground-state phase (see Fig. S2 [21]). These results indicate that the octahedral rotation types of all Ca-based bilayers remain unchanged with respect to their bulk phases [22]. This structural robustness may be related to their generally small tolerance factor. In contrast, the ground-state structures of most Sr-based bilayers exhibit $a^-a^-c^-$-type octahedral rotation with very slight tilt distortion. Therefore their structure and energy are close to that of the $a^0a^0c^-$-type octahedral rotation. Other structural phases, especially the $a^-a^-c^+$-type rotation, also compete for the ground state and even become the ground-state phase of a few Sr-based bilayers at specific U values. The change of U value causes the transition of the ground state of some Sr-based bilayers which are related to the energy proximity of different structural phases.

The $a^-a^-c^+$-type octahedral rotation results in a polar $P2_1$ phase. The polar displacements of the two surface layers are the same but opposite to that of the middle layer, resulting in a net polarization along the tilt axis. In contrast, in the nonpolar structure ($P\bar{1}$ space group) established by $a^-a^-c^-$-type octahedral rotation, an antipolar mode emerges and is coupled with the OR and tilt distortion. The polar displacements of the two surface layers are opposite, resulting in the cancellation of polarization. This so-called "hybrid improper antiferroelectricity" has recently been observed in layered perovskite oxides [23]. The above results indicate that octahedral rotation-induced polarization generally exists in the Ca-based bilayers.

Reversing the IR or tilt mode individually results in a reversal of polarization, both of which can be accomplished by a one-step or a multistep switching [13,24]. The multistep switching of reversing IR mode refers to changing the sense of rotation of each layer in turn, while the multistep switching of reversing tilt mode is accomplished by a 180° rotation of the tilt axis within the *ab* plane. The former undergoes a nonpolar intermediate state with $a^-a^-c^-$-type octahedral rotation, while the latter undergoes an orthorhombic twin state with its tilt axis perpendicular to the initial direction.

For all Ca-based bilayers, we evaluated their energy barrier of reversing polarization along different switching paths. The results show that the one-step switching paths that reverse the IR or tilt mode generally have a higher energy barrier because they respectively undergo a barrier phase without tilt or rotation distortion (see Fig. S3 [21]). For almost all bilayers considered, the multistep switching of reversing tilt mode (via an orthorhombic twin) has the lowest energy barrier (see Fig. S4 [21]). Previous experiments have shown that the emergence of orthorhombic twin domains in ferroelectric $Ca_3Ti_2O_7$ is responsible for its unexpectedly low switching barrier [25]. The multistep switching of reversing IR mode usually has a relatively high energy barrier due to the fact that it undergoes a barrier phase where the rotation of one perovskite layer disappears. However, for some bilayers it has close or even lower energy barrier compared with the multistep switching of reversing tilt mode (see Figs. S3 and S4 [21]). This indicates the possibility of ferroelectric switching via reversing the IR mode in this 2D polar system. The change of U value slightly modulates the energy barrier for most bilayers, but it may cause significant changes in the energy barrier and even the transition of the lowest-energy path for a few materials, such as the Co-containing bilayers, which tend to undergo a transition of spin states with the change of U values.

Then we calculated the total energy of various collinear magnetic orders to determine the magnetic ground states of the Ca-based bilayers. Electronic properties were also calculated based on the determined magnetic ground state (see Fig. S5 [21]). The ions at the beginning of the transition-metal series (containing Sc, Ti, Nb, Ta) are always nonmagnetic, while the subsequent Mo and W ions are also nonmagnetic, except for the specific combinations such as VMo, CrMo, FeMo, and CrW. Note that the Co ions in the CoNb and CoTa bilayers are transformed into a nonmagnetic state (at U_{20}) with the decrease of U values (see Fig. 2). The bilayers with only one type of magnetic ion are generally antiferromagnetic insulator. The exception appears in the ScRe and TiRu bilayers, whose magnetic ground state changes to ferromagnetic as the U value of the magnetic ions decreases. Most bilayers containing two types of magnetic ions exhibit a G-type antiferromagnetic phase, which results in ferrimagnetism due to the difference in magnetic moments of neighbor magnetic ions (see Fig. 2). However, the change of U value can cause the magnetic ground state of some bilayers to change from ferrimagnetic to antiferromagnetic (usually the C-type phase). A similar magnetic phase transition from G type to C type has been observed in some DP bulks [22,26], in which the magnetic exchange interaction is very sensitive to octahedral rotation distortion. Moreover, for some
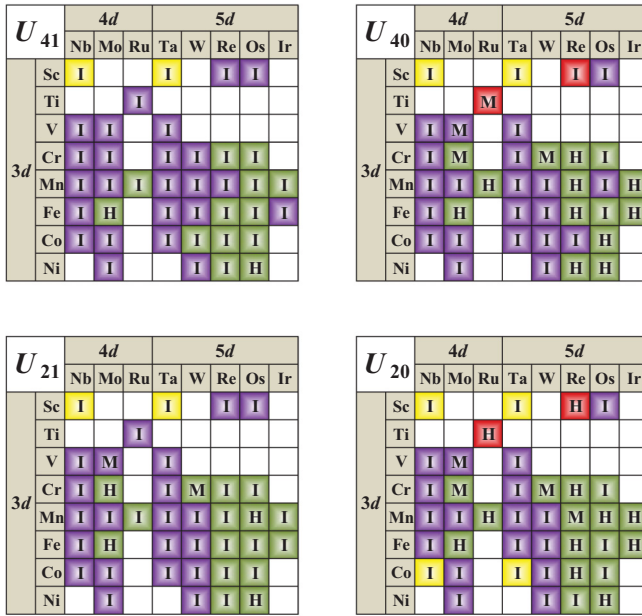
FIG. 2. Magnetic phases and electronic properties of Ca-based bilayers calculated with different U values. The effective U values used are $U_{3d} = 4$ eV, $U_{4d/5d} = 1$ eV (denoted as U_{41}), $U_{3d} = 4$ eV, $U_{4d/5d} = 0$ eV (U_{40}), $U_{3d} = 2$ eV, $U_{4d/5d} = 1$ eV (U_{21}), and $U_{3d} = 2$ eV, $U_{4d/5d} = 0$ eV (U_{20}), respectively. Color-filled squares represent the corresponding magnetic ground state: antiferromagnetic (purple), ferrimagnetic (green), ferromagnetic (red), and nonmagnetic (yellow). Capital letters denote the corresponding electronic properties: insulator (I), metal (M), and half-metal (H).

FIG. 3. (a) Magnetic anisotropy energy of the initial (**P**//**b**) and final (**P**//−**b**) states of ferroelectric switching for the Ca_3CrOsO_7 bilayer (U_{41}). The two final states are obtained by reversing rotation (IR) and tilt modes of the initial state, respectively. (b) Symmetry correlation between the crystal structures of the initial and final states. The curved solid arrows represent the directions of octahedral rotation and tilt distortion, and the dotted lines penetrating the octahedra represent the local easy-magnetization axes of the magnetic ions.

ferrimagnetic bilayers, the reduction in U values, especially for $4d$ and $5d$ ions, will lead to a transition from insulator to half-metal or metal. The metal-insulation transitions induced by the change of U value or temperature effect are common in DP bulks (especially those that contain Re) [27,28]. For most Ca-based bilayers, the electronic and magnetic properties calculated by nonzero U values of $4d/5d$ ions (U_{41} and U_{21}) remain unchanged with respect to their bulk phases (see Fig. S6 [21]).

These results indicate that the Ca-based DP bilayer system provides a broad platform for the realization of 2D multiferroics, polar ferromagnetic metals, and half-metals. Recent studies have shown that the polarization of polar metals can be switched via strain gradients [29], and even by electric fields in the 2D case [30,31]. Whether the in-plane polarization of the metal or half-metal bilayers can be switched needs to be further clarified.

Next, in order to identify the coupling between polarization and magnetization, we studied the change in the direction of magnetization with polarization reversal. Magnetic anisotropy calculation shows that the easy-magnetization axis always lies in the plane perpendicular to the tilt axis, which can be attributed to the twofold rotation symmetry around the tilt axis (see Supplemental Material [21]). Depending on whether the polarization is reversed by switching IR or tilt mode, the easy axis remains unchanged or rotates to a direction that is symmetric about the c axis with respect to the initial state, respectively [see Fig. 3(a)]. Although the Dzyaloshinskii-

Moriya interactions [32,33] may contribute significantly to the magnetic anisotropy of some bilayers (see Fig. S7 [21]), this transition of magnetization is material independent, as it is determined by the symmetric correlations. If the polarization is reversed through switching the IR mode, the crystal structures of the initial and final states are symmetrically correlated via an inversion symmetry and a mirror perpendicular to the tilt axis ($m \perp b$), which does not change the easy-axis direction [see Fig. 3(b)]. In contrast, when the polarization is reversed by switching the tilt mode, the initial and final states are symmetrically correlated via a twofold screw axis ($2_1//a$) and a twofold rotation symmetry ($2//c$). The directions of the local and global easy axes are changed in accordance with these symmetry operations.

However, given that there are two equivalent directions of magnetization along the easy axis, the ferroelectric switching by reversing IR mode may still cause the reversal of magnetization. Therefore we studied the evolution of the easy-axis direction along the switching paths of reversing IR mode. The easy axis always varies in the plane (ac plane) perpendicular to the tilt axis along the one-step switching path [see Fig. 4(a)], while it deviates from this plane during the multistep switching due to the absence of the twofold rotation symmetry [see Fig. 4(b)]. Whether following a one-step or multistep switching path, the evolution of magnetic anisotropy from the intermediate state to the final state is the inverse process from the initial state to the intermediate state. This is determined by the inversion symmetry correlation between the transition structures of the first half and the second half of the switching paths. Therefore, the magnetization will return to its initial direction when switching from the intermediate state to the final state, that is, the ferroelectric switching by reversing IR mode will not result in a reversal of the magnetization.
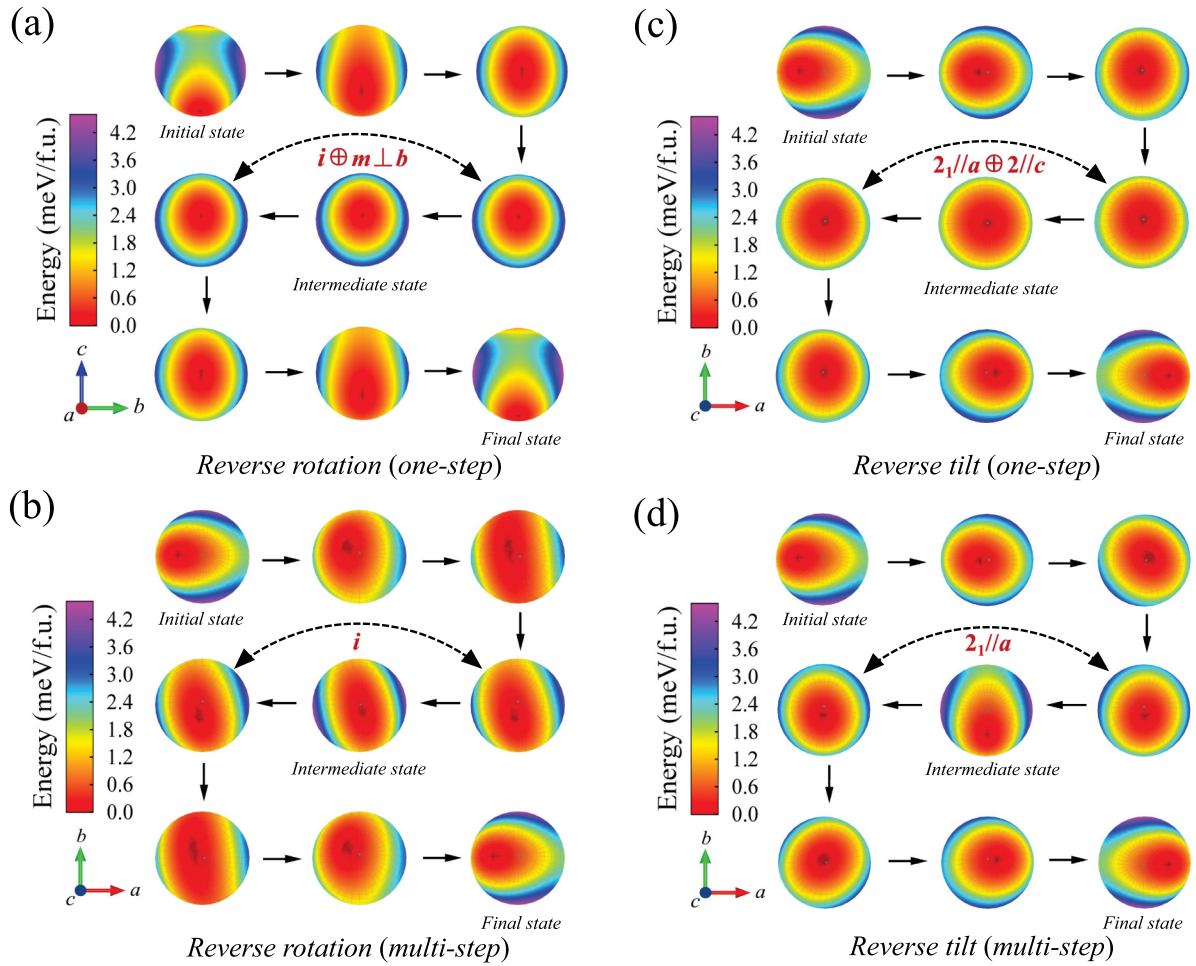
FIG. 4. Evolution of magnetic anisotropy energy surface along different ferroelectric switching paths for the Ca_3CrOsO_7 bilayer (U_{41}). The switching paths involve reversing the rotation mode through (a) a one-step or (b) a multistep switching and reversing the tilt mode through a (c) one-step or (d) multistep switching. The symmetry operation symbols describe the symmetry correlation between the corresponding transition structures of the first half (from the initial state to the intermediate state) and second half (from the intermediate state to the final state) of the switching paths.

For the ferroelectric switching by reversing tilt mode, the change in the easy-axis direction [see Fig. 3(a)] means that the in-plane or out-of-plane component of the magnetization will be reversed, depending on the specific evolution of the easy axis during the ferroelectric switching. Along the one-step switching path, the easy axis varies in the ac plane and transitions to the c axis in the intermediate state, and then rotates forward to a direction symmetrical about its initial direction [see Fig. 4(c)]. When following the multistep switching path, the easy axis rotates roughly around the c axis and passes through an orthogonal twin in the intermediate state [see Fig. 4(d)]. This change stems from the continuous rotation of the tilt axis in the ab plane. Whether following a one-step or multistep switching path, the magnetic anisotropy of the transition structures of the first half and the second half is mirror symmetrical ($m \perp a$), which is determined by the correlation of the twofold screw symmetry ($2_1//a$) between the corresponding transition structures. Therefore, as the polarization reverses through switching the tilt mode, the in-plane magnetization component will be reversed with the out-of-plane magnetization component unchanged. The above results

demonstrate that only the ferroelectric switching by reversing tilt mode can cause the change of the magnetization direction. Fortunately, the multistep switching path of reversing tilt mode generally has the lowest energy barrier, providing
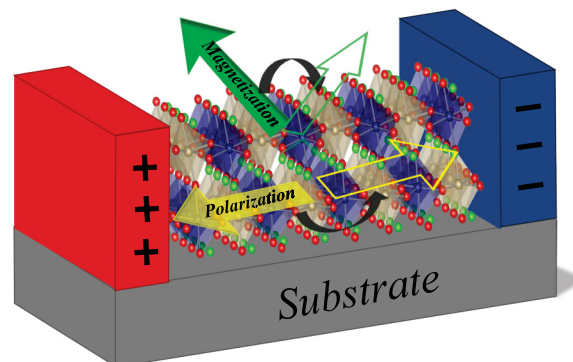
FIG. 5. Schematic diagram of switching the direction of magnetization by electric field.

a basis for realizing electric-field control of magnetization in this 2D system (see Fig. 5). In summary, our results show that 2D multiferroics widely exist in the Ca-based DP bilayer system, which also provides a broad platform for the design of 2D polar ferromagnetic metals and half-metals. The transition of magnetization induced by ferroelectric switching can be determined by analyzing the symmetry correlation between the initial and final polarization states. Reversing the rotation distortion does not change the direction of magnetization, while reversing the tilt distortion can lead to the reversal of the in-plane magnetization. This method, used to determine the

magnetoelectric coupling effect, can also be applied to other multiferroics systems.

[1] K. S. Novoselov, A. K. Geim, S. V. Morozov, D. Jiang, M. I. Katsnelson, I. V. Grigorieva, S. V. Dubonos, and A. A. Firsov, Nature (London) **438**, 197 (2005).

[2] A. H. Castro Neto, F. Guinea, N. M. R. Peres, K. S. Novoselov, and A. K. Geim, Rev. Mod. Phys. **81**, 109 (2009).

[3] A. Splendiani, L. Sun, Y. Zhang, T. Li, J. Kim, C.-Y. Chim, G. Galli, and F. Wang, Nano Lett. **10**, 1271 (2010).

[4] G. Wang, A. Chernikov, M. M. Glazov, T. F. Heinz, X. Marie, T. Amand, and B. Urbaszek, Rev. Mod. Phys. **90**, 021001 (2018).

[5] D. Xiao, G.-B. Liu, W. Feng, X. Xu, and W. Yao, Phys. Rev. Lett. **108**, 196802 (2012).

[6] H. Zhu, Y. Wang, J. Xiao, M. Liu, S. Xiong, Z. J. Wong, Z. Ye, Y. Ye, X. Yin, and X. Zhang, Nat. Nanotechnol. **10**, 151 (2014).

[7] G. R. Bhimanapati, Z. Lin, V. Meunier, Y. Jung, J. Cha, S. Das, D. Xiao, Y. Son, M. S. Strano, V. R. Cooper, L. Liang, S. G. Louie, E. Ringe, W. Zhou, S. S. Kim, R. R. Naik, B. G. Sumpter, H. Terrones, F. Xia, Y. Wang, J. Zhu, D. Akinwande, N. Alem, J. A. Schuller, R. E. Schaak, M. Terrones, and J. A. Robinson, ACS Nano **9**, 11509 (2015).

[8] S. S. Hong, J. H. Yu, D. Lu, A. F. Marshall, Y. Hikita, Y. Cui, and H. Y. Hwang, Sci. Adv. **3**, eaao5173 (2017).

[9] D. Ji, S. Cai, T. R. Paudel, H. Sun, C. Zhang, L. Han, Y. Wei, Y. Zang, M. Gu, Y. Zhang, W. Gao, H. Huyan, W. Guo, D. Wu, Z. Gu, E. Y. Tsymbal, P. Wang, Y. Nie, and X. Pan, Nature (London) **570**, 87 (2019).

[10] E. Dagotto, T. Hotta, and A. Moreo, Phys. Rep. **344**, 1 (2001).

[11] H. Akamatsu, K. Fujita, T. Kuge, A. Sen Gupta, A. Togo, S. Lei, F. Xue, G. Stone, J. M. Rondinelli, L.-Q. Chen, I. Tanaka, V. Gopalan, and K. Tanaka, Phys. Rev. Lett. **112**, 187602 (2014).

[12] J. Lu, W. Luo, J. Feng, and H. Xiang, Nano Lett. **18**, 595 (2017).

[13] J. Zhang, X. Shen, Y. Wang, C. Ji, Y. Zhou, J. Wang, F. Huang, and X. Lu, Phys. Rev. Lett. **125**, 017601 (2020).

[14] N. A. Benedek and C. J. Fennie, Phys. Rev. Lett. **106**, 107204 (2011).

[15] N. A. Benedek, A. T. Mulder, and C. J. Fennie, J. Solid State Chem. **195**, 11 (2012).

[16] J. M. Rondinelli and C. J. Fennie, Adv. Mater. **24**, 1961 (2012).

[17] P. V. Balachandran, J. Young, T. Lookman, and J. M. Rondinelli, Nat. Commun. **8**, 14282 (2017).

[18] I. Grinberg, D. V. West, M. Torres, G. Gou, D. M. Stein, L. Wu, G. Chen, E. M. Gallo, A. R. Akbashev, P. K. Davies, J. E. Spanier, and A. M. Rappe, Nature (London) **503**, 509 (2013).

[19] Y. Hu, F. Florio, Z. Chen, W. A. Phelan, M. A. Siegler, Z. Zhou, Y. Guo, R. Hawks, J. Jiang, J. Feng, L. Zhang, B. Wang, Y.

Wang, D. Gall, E. F. Palermo, Z. Lu, X. Sun, T.-M. Lu, H. Zhou, Y. Ren, E. Wertz, R. Sundararaman, and J. Shi, Sci. Adv. **6**, eaay4213 (2020).

[20] N. A. Spaldin and R. Ramesh, Nat. Mater. **18**, 203 (2019).

[21] See Supplemental Material at http://link.aps.org/supplemental/10.1103/PhysRevB.103.L220406 for computational details and results about the easy-axis direction, energy gain induced by structural distortion, phonon dispersion, and *abinitio* molecular dynamics simulation, energy barrier of ferroelectric switching, projected density of state, experimentally determined magnetic and electronic properties of some double-perovskite bulks, and magnetic anisotropy, which includes Refs. [22,28,34–46].

[22] S. Vasala and M. Karppinen, Prog. Solid State Chem. **43**, 1 (2015).

[23] S. Yoshida, K. Fujita, H. Akamatsu, O. Hernandez, A. S. Gupta, F. G. Brown, H. Padmanabhan, A. S. Gibbs, T. Kuge, R. Tsuji *et al.*, Adv. Funct. Mater. **28**, 1801856 (2018).

[24] E. A. Nowadnick and C. J. Fennie, Phys. Rev. B **94**, 104105 (2016).

[25] Y. S. Oh, X. Luo, F.-T. Huang, Y. Wang, and S.-W. Cheong, Nat. Mater. **14**, 407 (2015).

[26] R. Morrow, J. W. Freeland, and P. M. Woodward, Inorg. Chem. **53**, 7983 (2014).

[27] A. T. Lee and C. A. Marianetti, Phys. Rev. B **97**, 045102 (2018).

[28] H. Kato, T. Okuda, Y. Okimoto, Y. Tomioka, K. Oikawa, T. Kamiyama, and Y. Tokura, Phys. Rev. B **69**, 184412 (2004).

[29] A. Zabalo and M. Stengel, Phys. Rev. Lett. **126**, 127601 (2021).

[30] Z. Fei, W. Zhao, T. A. Palomaki, B. Sun, M. K. Miller, Z. Zhao, J. Yan, X. Xu, and D. H. Cobden, Nature (London) **560**, 336 (2018).

[31] J. Lu, G. Chen, W. Luo, J. Íñiguez, L. Bellaiche, and H. Xiang, Phys. Rev. Lett. **122**, 227601 (2019).

[32] I. Dzyaloshinsky, J. Phys. Chem. Solids **4**, 241 (1958).

[33] T. Moriya, Phys. Rev. **120**, 91 (1960).

[34] H. W. Eng, P. W. Barnes, B. M. Auer, and P. M. Woodward, J. Solid State Chem. **175**, 94 (2003).

[35] D. D. Russell, A. J. Neer, B. C. Melot, and S. Derakhshan, Inorg. Chem. **55**, 2240 (2016).

[36] J.-H. Choy, S.-T. Hong, and K.-S. Choi, J. Chem. Soc. Faraday Trans. **92**, 1051 (1996).

[37] R. Morrow, J. R. Soliz, A. J. Hauser, J. C. Gallagher, M. A. Susner, M. D. Sumption, A. A. Aczel, J. Yan, F. Yang, and P. M. Woodward, J. Solid State Chem. **238**, 46 (2016).

[38] J.-H. Choy, J.-H. Park, S.-T. Hong, and D.-K. Kim, J. Chem. Soc. Faraday Trans. **111**, 370 (1994).

[39] H. L. Feng, M. P. Ghimire, Z. Hu, S.-C. Liao, S. Agrestini, J. Chen, Y. Yuan, Y. Matsushita, Y. Tsujimoto, Y. Katsuya, M. Tanaka, H.-J. Lin, C.-T. Chen, S.-C. Weng, M. Valvidares, K. Chen, F. Baudelet, A. Tanaka, M. Greenblatt, L. H. Tjeng, and K. Yamaura, Phys. Rev. Mater. **3**, 124404 (2019).

[40] K. C. Kharkwal, R. Roy, H. Kumar, A. K. Bera, S. M. Yusuf, A. K. Shukla, K. Kumar, S. Kanungo, and A. K. Pramanik, Phys. Rev. B **102**, 174401 (2020).

[41] R. Morrow, K. Samanta, T. S. Dasgupta, J. Xiong, J. W. Freeland, D. Haskel, and P. M. Woodward, Chem. Mater. **28**, 3666 (2016).

[42] P. E. Blöchl, Phys. Rev. B **50**, 17953 (1994).

[43] G. Kresse and J. Furthmüller, Phys. Rev. B **54**, 11169 (1996).

[44] J. P. Perdew, A. Ruzsinszky, G. I. Csonka, O. A. Vydrov, G. E. Scuseria, L. A. Constantin, X. Zhou, and K. Burke, Phys. Rev. Lett. **100**, 136406 (2008).

[45] S. L. Dudarev, G. A. Botton, S. Y. Savrasov, C. J. Humphreys, and A. P. Sutton, Phys. Rev. B **57**, 1505 (1998).

[46] A. Neroni, E. Şaşıoğlu, H. Hadipour, C. Friedrich, S. Blügel, I. Mertig, and M. Ležaić, Phys. Rev. B **100**, 115113 (2019).